Accepted Manuscript

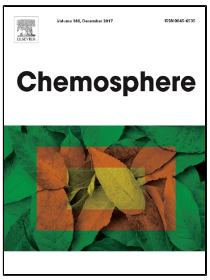

Biotrickling filter modeling for styrene abatement. Part 1: Model development, calibration and validation on an industrial scale

Pau San-Valero, Antonio D. Dorado, Vicente Martínez-Soria, Carmen Gabaldón

PII:	S0045-6535(17)31650-8
DOI:	10.1016/j.chemosphere.2017.10.069
Reference:	CHEM 20091
To appear in:	*Chemosphere*
Received Date:	09 June 2017
Revised Date:	21 September 2017
Accepted Date:	11 October 2017

Please cite this article as: Pau San-Valero, Antonio D. Dorado, Vicente Martínez-Soria, Carmen Gabaldón, Biotrickling filter modeling for styrene abatement. Part 1: Model development, calibration and validation on an industrial scale, *Chemosphere* (2017), doi: 10.1016/j.chemosphere.2017.10.069

Highlights

A dynamic model was applied for simulating styrene-degrading biotrickling filters

Discontinuous and fluctuating emissions and intermittent trickling were considered

The model was calibrated at laboratory with several inlet loadings conditions

The model also predicted the dynamic pattern of the outlet emission

Model was validated by 52 days of an on-site biotrickling under oscillating loading

Biotrickling filter modeling for styrene abatement. Part 1: Model development, calibration and validation on an industrial scale

Pau San-Valero[a], Antonio D. Dorado[b], Vicente Martínez-Soria[a], Carmen Gabaldón[a*]

[a] Research Group GI^{2}AM, Department of Chemical Engineering, Universitat de Valencia, Av. de la Universitat s/n, 46100 Burjassot, Spain. Tel. +34 963543437, Fax: +34 963544898

[b] Department of Mining Engineering and Natural Resources, Universitat Politècnica de Catalunya, Bases de Manresa 61-73,08240, Manresa, Spain

[*] Corresponding author: carmen.gabaldon@uv.es

Abstract

A three-phase dynamic mathematical model based on mass balances describing the main processes in biotrickling filtration: convection, mass transfer, diffusion, and biodegradation was calibrated and validated for the simulation of an industrial styrene-degrading biotrickling filter. The model considered the key features of the industrial operation of biotrickling filters: variable conditions of loading and intermittent irrigation. These features were included in the model switching from the mathematical description of periods with and without irrigation. Model equations were based on the mass balances describing the main processes in biotrickling filtration: convection, mass transfer, diffusion, and biodegradation. The model was calibrated with steady-state data from a laboratory biotrickling filter treating inlet loads at 13–74 g C m^{-3} h^{-1} and at empty bed residence time of 30–15 s. The model predicted the dynamic emission in the outlet of the biotrickling filter, simulating the small peaks of concentration occurring during irrigation. The validation of the model was performed using data from a pilot on-site biotrickling filter treating styrene installed in a fiber-reinforced facility. The model predicted the performance of the biotrickling filter working under high-oscillating emissions at an inlet load in a range of 5–23 g C m^{-3} h^{-1} and at an empty bed residence time of 31 s for more than 50 days, with a goodness of fit of 0.84.

Keywords: Biological air treatment; Biotrickling filter; Mathematical modeling; Styrene; Pilot unit; Volatile organic compound

1. Introduction

Styrene is one of the most widely used organic compounds because of its application as an intermediate product in industries that produce synthesized polymers and copolymers, such as polystyrene. Nevertheless, as a consequence of its physical properties (vapor pressure of 0.667 kPa at 20 ^{o}C), it is classified as a volatile organic compound (VOC), and thus its emissions to the atmosphere are strictly regulated (European Union, 2010). Styrene photochemical ozone creation was estimated at 14.2 (Derwent et al., 1998), and it was identified as reasonably anticipated to be a human carcinogen (National Toxicology Program (NTP), 2016). Therefore, companies should prioritize treating derivative styrene air emissions. Several efforts have been made to report styrene abatement. Traditionally, styrene air emissions are controlled by using a regenerative thermal or catalytic oxidizer. However, the treatment of styrene emissions using bioprocesses has been gaining attention from researchers in the last two decades (Lim et al., 2005; Lu, 2001; Pérez et al., 2015). In particular, biotrickling filtration technology has been demonstrated as a suitable alternative treating the air emissions of styrene (Pérez et al., 2015; Sempere et al., 2011) and to be feasible to replace conventional technologies. Moreover, biotrickling filters (BTFs) are cost-effective. The direct cost (excluding capital recovery) of treating styrene air emissions has been reported to be more than three times lower than that of regenerative catalytic oxidization combined with a zeolite pre-concentrator (Álvarez-Hornos et al., 2017).

Industrial air emissions of any facility are characterized by fluctuating conditions of inlet concentrations and gas flow rates related to the random variations in the manufacturing processes and short off closures during weekends. Therefore, industrial BTFs can exhibit a different performance than that observed at the laboratory, and the influence of these dynamic variations on BTFs is one of the current issues of interest.

Only a few studies on the pilot-industrial scale (Álvarez-Hornos et al., 2017; Webster et al., 1999) are available, thus making it difficult to achieve a real consolidation of the bioprocess in the industrial field. One of the earlier studies on the pilot/full-scale BTF reactor applied to styrene treatment was conducted in 1999 by Webster et al. (1999), and it assessed several operational problems. In their study, the pilot BTF treated inlet concentrations up to 0.8 g m^{-3} (empty bed residence time (EBRT) of 86 s) with an elimination capacity (EC) of 24 g m^{-3} h^{-1} and 70–85 % removal efficiency (RE). However, the authors encountered that transient conditions led to unstable biofilm as well as biological and mass transfer limitations. More recently, Álvarez-Hornos et al. (2017) demonstrated the feasibility of a BTF to treat styrene air emissions from a fiber-reinforced plastic industry with a maximum EC of 18.8 g m^{-3} h^{-1} (an RE of 75.6%, an EBRT of 31 s, and an inlet concentration of 0.21 g m^{-3}). Note that this application was performed under conditions of intermittent irrigation, which is the common operational protocol in the industry (Álvarez-Hornos et al., 2017; Deshusses and Webster, 2000; Lafita et al., 2012). Intermittent recycling water has been demonstrated as an advantageous operation strategy in terms of economic savings associated with energy costs and processes (Deshusses and Webster, 2000; Sempere et al., 2008).

Researchers in the field agree that mathematical modeling is useful to improve the knowledge about bioprocesses, to understand the effect of the variations of the operational parameters, and to predict the overall performance of the system, thus avoiding the excessive consumption of time and resources (Alonso et al., 1998; Okkerse et al., 1999; Zarook et al., 1997). Traditionally, phenomenological models have been used to simulate biofilters (Álvarez-Hornos et al., 2009; Das et al., 2011), BTFs (Kim and Deshusses, 2003), and trickled bed biofilters (Liao et al., 2008). These configurations are usually described by steps in a series (gas–liquid–biofilm) based on

the mass balances including the main mechanisms, such as diffusion, mass transfer, and kinetics (Devinny and Ramesh, 2005). Although this approach is a well-accepted common framework and has been demonstrated as a good approximation (Arellano-García et al., 2015; Baltzis et al., 2001; Dorado et al., 2012, 2008; Mpanias and Baltzis, 1998), its expandability to industrial applications is still scarce, due to the difficulty to obtain a reliable set of data.

This work aimed to apply a dynamic mathematical model to simulate the performance of an on-site BTF treating styrene emissions under oscillating inlet concentrations and operated under intermittent spraying, a common industrial protocol. The model was adapted on the basis of the one proposed by San-Valero et al. (2015) for isopropanol (a highly soluble compound); this model was initially created for simulating systems with variable inlet concentration patterns and gas flow rates, and with cyclic conditions between irrigation and non-irrigation periods. The model was calibrated with laboratory data on a BTF degrading styrene for 75 days (San-Valero et al., 2017). Afterwards, the model was validated by predicting the performance of almost two months of operation of a pilot BTF working in a fiber-reinforced facility (Álvarez-Hornos et al., 2017). This work appears as a first attempt to model the dynamic response of an industrial BTF treating variable styrene emissions, thus contributing to the development of predictive tools for helping practitioners to expand the application of biotrickling filtration to industry.

2. Materials and Methods

2.1. Lab-scale BTF operation

The lab-scale BTF consisted of a cylindrical column (0.144 m inner diameter, 1.63 m height) with a working packed volume of 20 L (working height: 1.23 m) coupled to an external recirculation tank with a 6 L capacity for column irrigation. The BTF was filled

114 with polypropylene rings with a 25 mm nominal diameter and 207 m^2 m^{-3} surface area
115 (a) with 92% void fraction (θ_P) (Flexiring®, Koch-Glitsch B.V.B.A., Belgium). The
116 liquid phase was intermittently irrigated from the recirculation tank by a centrifugal
117 pump with a frequency of irrigation of 15 min every 2 h. The liquid flow rate was set at
118 2.7 L min^{-1}, which is equivalent to a liquid velocity of 10 m h^{-1}. The air stream was
119 doped with styrene using a syringe pump (New Era, NE 1000 model, USA) at
120 concentrations of 0.18–0.32 g C m^{-3}. The gas flow rate was adjusted by a mass flow
121 controller (Bronkhorst Hi-Tec, the Netherlands) in the range of 2.4–4.8 m^3 h^{-1}
122 depending on the operation period. During the BTF operation, the inlet load (IL)
123 increased from 22 g C m^{-3} h^{-1} up to 43 g C m^{-3} h^{-1} by decreasing the EBRT from 30 s to
124 15 s. Subsequently, the EBRT was maintained at 15 s and the inlet concentration was
125 set to obtain ILs of 13–74 g C m^{-3} h^{-1}. The selected conditions for calibration purposes
126 are compiled in Table 1, corresponding to the average daily data representing the stable
127 conditions of the BTF performance. The purge of 3 L of the recirculation tank was
128 carried out once per week, and it represented less than 3% of carbon fed to the reactor
129 during the week. Further details can be found in San-Valero et al. (2017).
130
131 Table 1. Experimental data used for the calibration of the BTF model (San-Valero et al.,
132 2017). ± represents standard deviation

Days	IL (g C m^{-3} h^{-1})	Inlet conc. (mg C m^{-3})	EBRT (s)	EC (g C m^{-3} h^{-1})
15-36	22	184	30	20.5 ± 1.1
42-47	33	184	20	21.1± 1.6
50-60	43	181	15	17.9 ± 3.1
63-67	23	98	15	9.4 ± 2.3
68-70	74	312	15	27.5 ± 4.2
71-75	13	55	15	7.9 ± 0.9

133
134

135

136 2.2. On-site pilot BTF operation

137 The pilot scale BTF (VOCUS®, Pas Solutions BV, the Netherlands) consisted of a
138 packed reactor, which has an effective volume of 0.6 m^3 and is filled with a structured
139 packing material (PAS Winded Media) with a void space of 93 %, a specific surface
140 area of 410 $m^2 m^{-3}$, and a recirculation tank of 0.4 m^3. Part of the industrial emission
141 was fed to the BTF using a blower and a variable frequency drive. The BTF was
142 operated in a counter-current mode, the polluted air stream was blown at the bottom of
143 the column, and the recirculated water was intermittently irrigated (10 min per hour) on
144 the top at a flow rate of 2.7 $m^{-3} h^{-1}$. The BTF unit was operated for more than one year
145 with EBRTs varying between 31 s and 66 s. For modeling purposes, the last 52 days of
146 operation were chosen as representatives of a stable biofilm. In this period, the reactor
147 was operated at daily average ILs at 6–25 g styrene $m^{-3} h^{-1}$ (5–23 g C $m^{-3} h^{-1}$) and at a
148 constant EBRT of 31 s.

149 2.3. Model description

150 The dynamic model of this study was previously applied by San-Valero et al. (2015) for
151 isopropanol removal. The model includes two components, a pollutant (in this case,
152 styrene) and oxygen, and considers irrigation and non-irrigation periods. The model
153 considers the following well-accepted assumptions in the field:

154 (1) The gas phase flowed in a plug flow regime along the filter bed, thus neglecting
155 axial dispersion.

156 (2) The adsorption of pollutants in the packing material was negligible.

157 (3) The packing material was completely covered by a biofilm, which was
158 completely covered by the liquid phase.

159 (4) The gas–liquid interface was in equilibrium according to Henry's law.

(5) Biodegradation took place only in the biofilm.

The model equations are summarized as follows (*i* denotes styrene or oxygen):

Mass balance in the gas phase

$$\theta_G \frac{\partial C_{G_i}}{\partial t} = -v_G \frac{\partial C_{G_i}}{\partial z} - K_L a_i \left(\frac{C_{G_i}}{H_i} - C_{L_i} \right) \qquad (1)$$

Mass balance in the liquid phase

$$\theta_L \frac{\partial C_{L_i}}{\partial t} = v_L \frac{\partial C_{L_i}}{\partial z} + K_L a_i \left(\frac{C_{G_i}}{H_i} - C_{L_i} \right) - \frac{D_i a}{\beta} (C_{L_i} - S_{i,1}) \qquad (2)$$

Mass balance in the biofilm

$$\frac{\partial S_i}{\partial t} = f(X_v) D_i \frac{\partial^2 S_i}{\partial x^2} - \frac{\mu_{\max} X_v}{Y_i} \frac{S_{sty}}{S_{sty} + K_{sty}} \frac{S_O}{S_O + K_O} \qquad (3)$$

During periods of irrigation, the mass balances were described as follows: styrene and oxygen from the gas phase circulate through the column by considering the convective transport. Styrene and oxygen are transferred to the liquid phase, with the mass flux at the gas–liquid interface described by the global mass transfer coefficients ($K_L a_i$). The mass balance of the mobile liquid phase is produced by the circulation of the liquid phase in the counter-current mode with the gas phase, which is described by the convective transport equation. The liquid concentration at the top of the column is the result of the mass balance in the recirculation tank considering ideal stirring during irrigation and no biodegradation:

$$\frac{\partial C_{L_i}}{\partial t} = \frac{Q_L}{V_T} (C_{L_{i_{z=0}}} - C_{L_{i_{z=Z}}}) \qquad (4)$$

The mass transfer from liquid to biofilm of both components is a function of the specific surface area of the packing material (a), the diffusion coefficient in water (D_i), and the thickness of the liquid film (β). In the biofilm, diffusion and biodegradation take

181 place simultaneously; the former is described by Fick's second law and the latter by a
182 Monod expression including oxygen limitation.
183 During non-irrigation periods, the liquid phase is considered a stagnant phase without
184 dynamic hold-up, so there is no convective transport (v_L=0), and the pollutant
185 concentration of the recirculating water remains constant. The main difference with
186 respect to San-Valero et al. (2015) is the phenomenon accounting for the mass transfer
187 from the gas phase to the stagnant liquid. It was demonstrated that in the case of high
188 water-soluble compounds, the stagnant phase serves as a pollutant sink (mass transfer
189 resistance negligible). In the case of styrene, it was assumed that the resistance of the
190 stagnant liquid is the same than that of during irrigation.
191 2.4. Numerical resolution
192 The partial differential equations were two second-order nonlinear distributed systems.
193 The method of lines (MOL) was applied to solve the systems by generating a uniform
194 grid in the spatial dimensions: the height of the reactor and the biofilm thickness. For
195 each node, the partial derivatives were replaced by finite difference approximations.
196 The optimal discretization in terms of the result and time computing was 10 sections
197 along the bed (11 nodes) and 20 sections in the biofilm (21 nodes). Increasing the
198 discretization did not produced substantial variations on the model estimation. The set
199 of differential equations was solved with the implicit integration method from
200 MATLAB®, ode23t, which is the implementation of the trapezoidal rule using a free
201 interpolant and is especially suitable to moderately stiff systems.
202 The execution of the model was implemented in MATLAB® by creating a graphical
203 user interface (GUI-MATLAB®) to allow specifying variable gas and inlet
204 concentration patterns, as well as the duration and frequency of the spraying cycles.

Further details can be found elsewhere (San-Valero et al., 2016). A conceptual scheme of the model resolution is shown in Fig. 1.

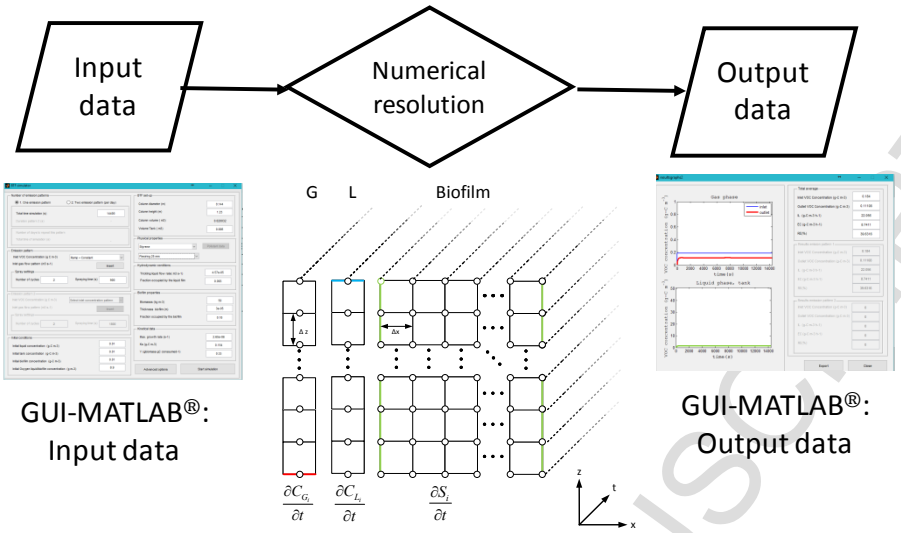

Fig. 1. Conceptual scheme of the model implementation and resolution.

The overall gas–liquid mass transfer coefficient of styrene and the maximum growth rate were determined by the calibration of the model to the experimental data by minimizing the objective function (OF), which was defined as the sum of the norm of the deviation between the RE predicted by the model (RE_{mod}) and the experimental one (RE_{exp}):

$$OF = \sum_{i=1}^{N} \left(norm\left(RE_{\text{mod}} - RE_{\text{exp}} \right) \right) \quad (5)$$

The parameter estimation was conducted by a MATLAB® algorithm, *fminsearch*, which consisted of searching the minimum of the unconstrained multivariable function using the simplex search method proposed by Lagarias et al. (1998). This direct search method does not use numerical or analytic gradients.

3. Results

3.1 Model calibration

The calibration of the dynamic model was performed with data from a styrene-degrading BTF operated at variable EBRTs and ILs (San-Valero et al., 2017). The

results correspond to the average data at the end of each operational condition tested (Table 1) when the BTF achieved stable performance.

The global gas–liquid mass transfer coefficient of styrene (K_La_{sty}) and the maximum growth rate (μ_{max}) were chosen as the calibration parameters. Parnian et al. (2016) determined the mass transfer coefficient of styrene in an abiotic BTF packed with pumice grains and steel pall rings. They found an increase in the K_La from 54–70 h^{-1} at 30ºC on the countercurrent gas-to-liquid flow ratio that varied in the range of 7.5–32, with a potential dependence. The variation in the gas-to-liquid flow ratio in this study was in a narrow range from 16–31 and at room temperature; thus, both factors (the gas-to-liquid flow ratio and temperature) seem to indicate that variations should be lower than 11%. The influence of EBRT on K_La was considered negligible in the tested range in comparison with the inherent simplicity of the model to represent the complex phenomena occurring in a BTF (e.g., uneven wetted biofilm, irregular biofilm growth, etc.).

The rest of the model parameters are shown in Table 2. The physicochemical parameters were taken from the literature (Fan et al., 1990; Reid et al., 1987; Sander, 2005), except the overall mass-transfer coefficient for oxygen, which was estimated from previous experiments (San-Valero et al., 2014). Among the kinetic parameters, the yield coefficient of styrene was estimated from the CO_2 production reported by Sempere et al. (2011), and the yield coefficient of oxygen was stoichiometrically calculated. Half-saturation constants were taken from literature (Jung and Park, 2005; Shareefdeen et al., 1993). Biofilm and liquid properties (biofilm thickness (δ), liquid film thickness (β), and biofilm properties (X_v, θ_B)) were taken from our previous work, in which the model was calibrated using the same experimental setup as the removal of

247 isopropanol emissions in air by BTF (San-Valero et al., 2015), except for the fraction
248 occupied by the liquid film (θ_L), which was experimentally determined.
249 The calibration procedure based on the minimization of the OF defined in Eq. 5 resulted
250 in a global mass transfer coefficient of styrene of 1.14×10^{-2} s^{-1} and a maximum growth
251 rate of 2.65×10^{-6} s^{-1}. The value of the global mass transfer coefficient of styrene (41 h^{-1})
252 is in agreement with the order of magnitude expected from the values of Parnian et al.
253 (2016) considering the differences in the operational conditions. The values of the
254 maximum growth rate of the same order of magnitude were previously reported in
255 biofilters treating styrene (Jorio et al., 2005, 2003).
256
257 Table 2: BTF model parameters

	Specific Value	**Reference**
Physicochemical parameters		
D_{sty} (m^2 **s^{-1}**)	8.97×10^{-10}	(Reid et al., 1987)
D_O (m^2 **s^{-1}**)	2.0×10^{-9}	(Reid et al., 1987)
f(Xv)	0.35	(Fan et al., 1990)
H_{sty}	0.1	(Sander, 2005)
H_O	31.4	(Sander, 2005)
$K_L a_O$ **(s^{-1})**	0.013	This work
Kinetical data		
Ko ($g\ m^{-3}$)	0.26	(Shareefdeen et al., 1993)
Y_{sty}	0.33	This work
Yo	0.12	Stoichiometric balance
K_{sty} ($g\ m^{-3}$)	0.154	(Jung and Park, 2005)
Biofilm and liquid film properties		
δ (m)	60×10^{-6}	(San-Valero et al., 2015)
β (m)	3.8×10^{-6}	(San-Valero et al., 2015)
X_v ($kg\ m^{-3}$)	50	(San-Valero et al., 2015)
θ_L	0.093	This work
θ_B	0.18	(San-Valero et al., 2015)

258
259 The good agreement between the model predictions and the experimental data in the
260 calibration step is shown in Fig. 2, in which the relationship between the modeled and

261 the experimental EC is plotted for the three tested EBRTs (15, 20, and 30 s). The model
262 prediction fit the experimental data with deviations below ± 20% of the relative error.
263 Statistical analysis was conducted and revealed a correlation between the modeled and
264 the experimental EC with a goodness of fit of 0.84 using the normalized mean square
265 error. The greatest deviations (23%) were obtained at the ILs of 23 g C m^{-3} h^{-1} (EBRT
266 =15 s) and 22 g C m^{-3} h^{-1} (EBRT =30 s). In the first case, the modeled EC was 11.5 g C
267 m^{-3} h^{-1} versus the experimental EC at 9.4 ± 2.3 g C m^{-3} h^{-1}. Therefore, the EC predicted
268 by the model was within the error experimentally observed. In the second case, the
269 model underestimated the experimental value of the EC from 20.4 ± 1.1 g C m^{-3} h^{-1} to
270 15.7 g C m^{-3} h^{-1}, as predicted by the model. Note that this deviation coincided with the
271 start-up of the BTF, and it may be attributed to the fact that the biofilm properties in this
272 stage could be under evolution. The RE achieved by the model (72%) is close to the
273 other experimental data achieved with mature biofilms. For example, Pérez et al. (2015)
274 obtained an RE of 75–80 % using the same EBRT (30 s), a similar IL (22 g m^{-3} h^{-1}), and
275 the same irrigation frequency after more than 130 days from start-up.

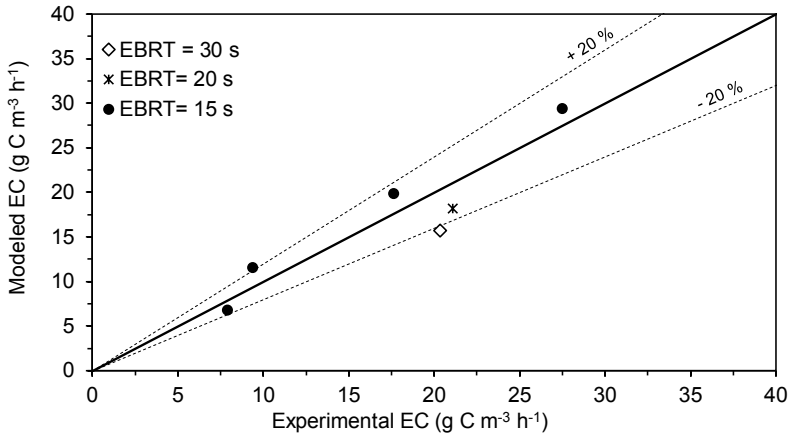

276

277 Fig. 2: Comparison between the experimental and the modeled EC of the laboratory
278 BTF from the model calibration

279 To evaluate whether the model could predict the variation in EC caused by the increase
280 in the IL, simulations were performed for the conditions experimentally tested at an

281 EBRT of 15 s (Fig. 3). The model accurately predicted the variation in EC caused by
282 the increase in the IL. At 15 s, the BTF did not achieve a complete degradation of
283 styrene at any IL tested. However, an increase in the IL led to an increase in the EC.
284 Thus, it seems to indicate that the mass transfer limited the system instead of the
285 biodegradation kinetic, as the microorganisms were able to remove more styrene if it is
286 transferred to the biofilm. In this regard, the model was able to reproduce the
287 characteristic curve of the BTF performance and to predict the limits of the application
288 of this technology for styrene abatement. The experimental maximum EC was 28 ± 4 g
289 C m^{-3} h^{-1}, and the model predicted a maximum EC of 29 g C m^{-3} h^{-1}, which was within
290 the experimental error.

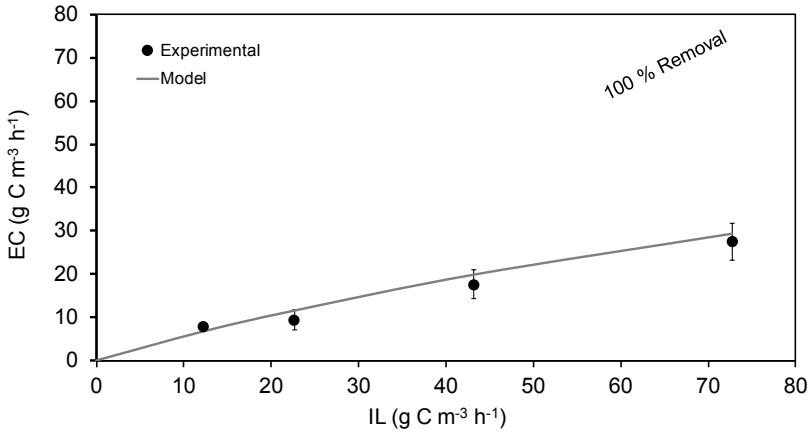

291

292 Fig. 3: Model prediction of the relationship between the EC and the IL of the laboratory
293 BTF working at an EBRT of 15 s

294 Aside from modeling a satisfactorily steady-state operation, the model predicted with a
295 high level of correspondence the continuous monitoring of the gas phase styrene
296 concentration influenced by the cycles of irrigation on a complete day of operation (Fig.
297 4a, experiment IL = 22 g C m^{-3} h^{-1}, EBRT = 30 s). For a daily average outlet
298 concentration in the gas phase lower than 50 mg C m^{-3}, the pattern emission showed
299 small peaks of styrene (from 21 up to 35 mg C m^{-3}) matching with the irrigation
300 periods, creating a clear dynamic pattern. The model predicted the occurrence of these

perturbations (peaks of pollutant during irrigation) with the same duration by considering the cycling between irrigation and non-irrigation periods, which is a remarkable operation parameter in industrial BTFs. In the case of a daily average outlet concentration of ~70 mg C m^{-3}, the perturbation of the spraying is not noticeable in comparison with the instantaneous variations (Fig 4b, experiment IL = 33 g C m^{-3} h^{-1}, EBRT = 20 s). The capability of the model to reproduce a dynamic pattern on an industrial scale is important to evaluate its effect, which can be optimized in the function of the target pollutant. For styrene, it seems that irrigation frequency could be increased or diminished in the function of the needs of operational parameters, such as nutrients, pH, or pressure drop, without adversely impacting the daily averaged removal efficiency.

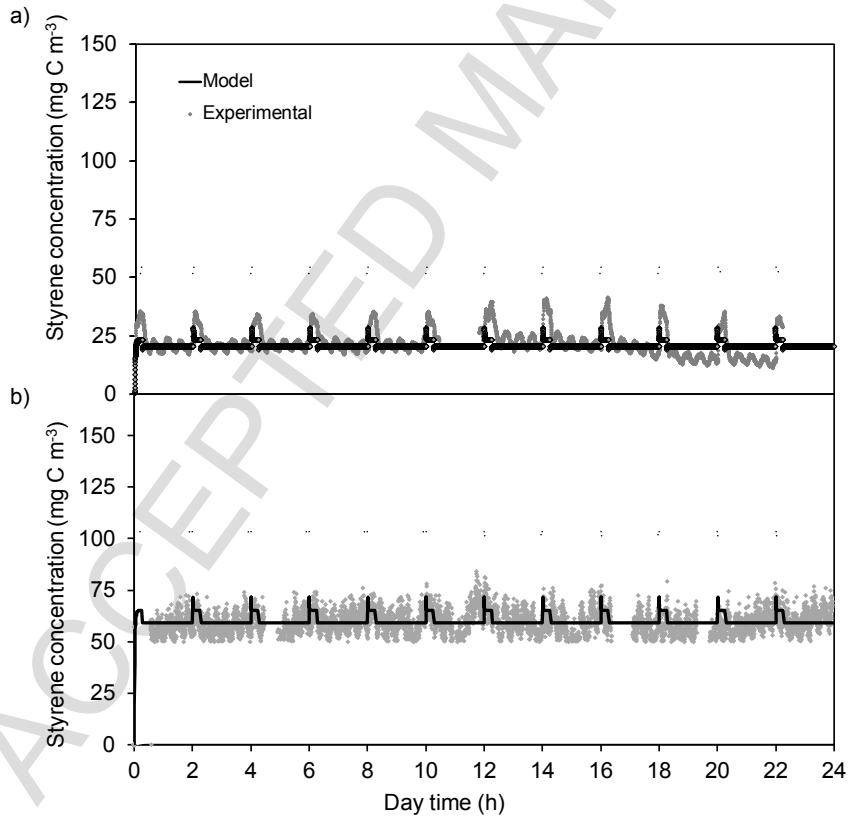

Fig. 4: Experimental pattern and model predictions corresponding to the instantaneous outlet styrene concentration of the laboratory BTF: a) IL = 22 g C m^{-3} h^{-1}, EBRT = 30 s b) IL = 33 g C m^{-3} h^{-1}, EBRT = 20 s. Arrows denote 15 min of spraying.

316 A different behavior was observed for isopropanol under an irrigation/non-irrigation
317 cyclic operation: a complete removal was attained during non-irrigation, while peaks of
318 high outlet concentrations (40–50% of inlet concentrations) were observed during
319 irrigation. The decrease in irrigation frequency from 15 min every 1.5 h to 15 min every
320 3 h caused a decrease in the daily average outlet concentrations from 86–59 mg C Nm^{-3}
321 (San-Valero et al., 2013). The fact that both pollutants show different behavior during
322 non-irrigation periods is noteworthy. In the treatment of isopropanol, a complete
323 removal was attained during periods without irrigation, demonstrating that the
324 resistance to mass transfer of the stagnant liquid phase was negligible compared with
325 that occurring during periods with irrigation. In contrast, a similar mass transfer
326 resistance of the mobile liquid (irrigation) and the stagnant liquid (non-irrigation)
327 reproduces in large extent the dynamic pattern of styrene emissions. This result shows
328 the applicability of the model to pollutants with different affinities to water.

329 3.2 Model sensitivity

330 The sensitivity of the model was evaluated comparing the relative changes in the outlet
331 concentration by the variation of 50% of the mass transfer coefficient of styrene (K_La_{sty}),
332 kinetic parameters (μ_{max}, K_{sty}), biofilm thickness (δ), liquid thickness (β) diffusivity of
333 styrene (D_{sty}), and Henry law's constant of styrene (H_{sty}). The sensitivity of the model to
334 each parameter was carried out following that proposed by Baquerizo et al. (2005):

$$sensitivity = \frac{\frac{\Delta C_G^{out}}{C_{G_d}^{out}}}{\left|\frac{\Delta p}{p_d}\right|} \quad (6)$$

335

336 where C_G^{out} is the outlet concentration of the gas phase and p is the evaluated parameter.
337 Subscript d refers to the default values. The analysis was performed using the operational

conditions corresponding to an IL of 22 g C m^{-3} h^{-1} and an EBRT of 30 s. The results are shown in Table 3.

Table 3: Sensitivity analysis of the BTF model

Parameter	Δ (%)	Sensitivity, C_G^{out}
K_La_{sty}	- 50	0.699
	+ 50	-0.226
μ_{max}	- 50	0.792
	+ 50	-0.340
K_{sty}	- 50	-0.189
	+ 50	0.113
δ	- 50	2.151
	+ 50	-0.642
β	- 50	-1.094
	+ 50	0.868
D_{sty}	- 50	0.770
	+ 50	-0.377
H_{sty}	-50	-1.175
	+ 50	0.830

As shown in Table 3, the model was sensitive to the physicochemical parameters. The most sensitive value was found for low values of biofilm thickness. The analysis also revealed that the liquid thickness, the Henry's law constant, the mass transfer coefficient of styrene, and the diffusion coefficient of styrene had a notable impact on model predictions. Regarding the kinetic parameters, the most sensitive was the maximum growth rate. This finding is consistent with that reported in previous literature. For example, Baquerizo et al. (2005) found that specific biofilm thickness and specific surface area (here lumped by β and K_La) were the most sensitive parameters in the modeling of a biofilter for ammonia removal.

3.3 Model validation at on-site pilot BTF

The model validation was conducted using the experimental data from the pilot BTF installed in a fiber-reinforced plastic industry that treats styrene for more than one year. The average daily data on the pilot BTF operated at a constant EBRT of 31 s and

355 variable ILs of 5–23 g C m^{-3} h^{-1} were compiled. This set of data was recommended by
356 the authors for scale-up purposes and considered to be representative of an active and
357 stable biofilm (Álvarez-Hornos et al., 2017). In the pilot testing, the styrene
358 concentration in the inlet air fluctuated from 40 mg Nm^{-3} to 350 mg Nm^{-3} associated
359 with the fluctuations in the manufacturing processes of the factory. As an illustrative
360 example, Fig. 5 shows a typical emission on one day. However, as the average daily
361 concentration was the only data available, the inlet concentration was considered
362 constant during the day for modeling purposes. When the inlet concentration was not
363 available during one day, IL was approximated as a piecewise step between the two
364 closest times.

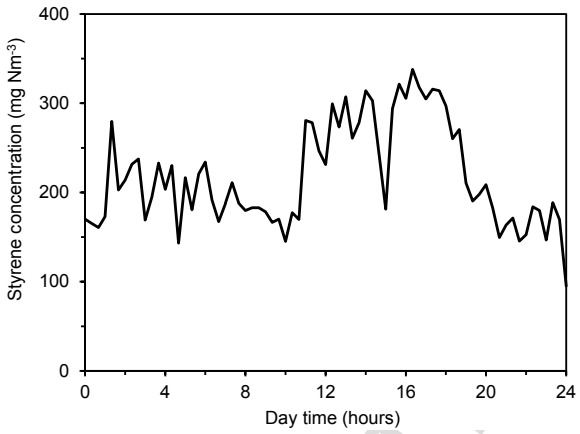

365

366 Fig. 5: Typical fluctuations of styrene concentrations in the air emissions treated by the
367 pilot BTF installed in a fiber-reinforced plastic industry

368 The model was applied using the parameters listed in Table 2, except for the physical
369 properties corresponding to the packing material used in this setup, which is different
370 from that used at laboratory experiments (a=410 m^2 m^{-3}, θ_P=93%) and the overall mass
371 transfer coefficient of oxygen ($K_L a_O$= 0.0121 s^{-1}), which was determined by the
372 correlation specifically developed for this packing as proposed in San-Valero et al.
373 (2014). Fig. 6 depicts the experimental IL and EC as the data points along with the
374 model ones (continuous line). The data obtained by the model corresponded to the

instantaneous variations (order of seconds), thus resulting in small oscillations in the EC plots associated with the irrigation effect on the outlet emission. This transitory effect could be considered negligible in terms of the average daily EC. The goodness of fit of the model and the experimental data was 0.84 according to the normalized mean square error. The model was able to successfully represent the on-site pilot BTF under transient conditions of loading. For example, on day 23 the model predicted an EC of ~15 g C m^{-3} h^{-1} at an IL of ~18 g C m^{-3} h^{-1}; on the next day the EC decreased until ~5.0 g C m^{-3} h^{-1} at IL of ~5.6 g C m^{-3} h^{-1}. The simulation of the model enabled the prediction of the overall performance of an industrial installation for a period over 50 days with significant correspondence. The slight deviations between the model predictions and the experimental data could be attributed to the fact that the simulations were conducted using the average daily IL rather than the instantaneous fluctuations of the industrial emission (Fig. 5).

The model reproduced the performance of the BTFs on both laboratory and on-site pilot scales by applying the same phenomena and using the same biofilm thickness. This did not occur during the treatment of hydrophilic compounds, in which experimental evidence supported by model predictions confirmed an excessive and uncontrolled biofilm growth on the industrial scale compared with that of the laboratory scale (San-Valero et al., 2015). The results obtained in this work seem to indicate that the removal of industrial emissions of moderately hydrophobic compounds, such as styrene, by BTFs could be characterized by slow biofilm growth. Previous authors have observed that styrene abatement at industrial sites could lead to difficulties in establishing a stable biofilm in the short term in industrial installation (Álvarez-Hornos et al., 2017; Webster et al., 1999). However, when stable biofilm is established, slow biofilm growth could benefit the long-term performance of the industrial unit, achieving an RE similar to that

of the laboratory unit, and minimizing other operational problems, such as clogging or pollutant accumulation within the biofilm.

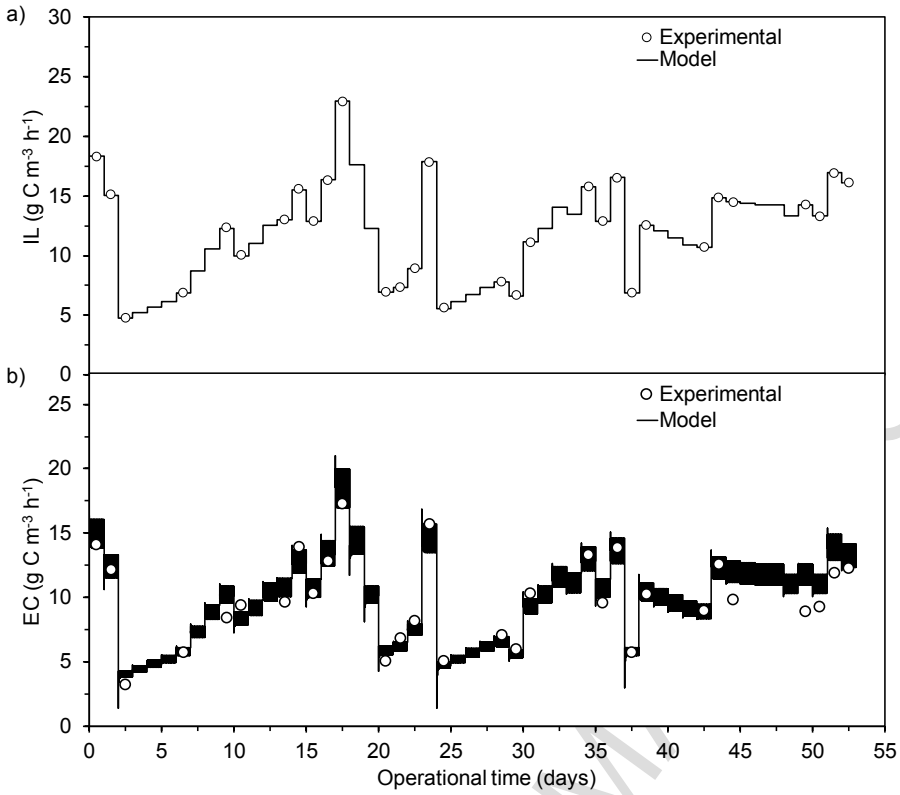

Fig. 6: Experimental evolution of the on-site BTF installed in a fiber-reinforced plastic industry along with the model simulations: a) IL; b) EC.

The approach considered in the development of this model, which was fitted by the calibration of only two parameters, $K_L a_{sty}$ and μ_{max}, was valid to represent the phenomena occurring in the treatment of styrene by BTFs in the laboratory and at industrial scale, and in steady and dynamic conditions, improving the knowledge about the rate-limiting step of the process. From a practical point of view, this approach can be used by practitioners in the design and operation of industrial BTFs treating styrene and other pollutants by adapting the related parameters. The developed model herein is the base to predict and evaluate styrene abatement under new and promising bioreactor configurations, such as a two-phase partitioning bioreactor, which is potentially interesting for low-soluble compounds such as styrene (see part 2).

4. Conclusions

A dynamic model to simulate a styrene-degrading laboratory BTF was developed through a set of differential equations switching from irrigation to non-irrigation periods by implementing in a graphical user interface (GUI-MATLAB®). The results obtained herein with those results previously on modeling the isopropanol emissions under cyclic irrigation/non-irrigation periods are of interest to show that the rate-limiting step of the process depends on the water solubility of the compound. The daily average elimination capacity of a pilot BTF installed in a fiber-reinforced plastic industry working under oscillating inlet concentrations and loading was successfully simulated, thus showing the robustness of the model as a predictive tool.

Acknowledgments

The authors acknowledge the financial support of the Ministerio de Economía y Competitividad (Project CTM2014-54517-R with FEDER funds) and Generalitat Valenciana (PROMETEO/2013/053), Spain.

References

Alonso, C., Suidan, M.T., Kim, B.R., Kim, B.J., 1998. Dynamic mathematical model for the biodegradation of VOCs in a biofilter: biomass accumulation study. Environ. Sci. Technol. 32, 3118–3123. doi:10.1021/es9711021

Álvarez-Hornos, F.J., Gabaldón, C., Martínez-Soria, V., Marzal, P., Penya-roja, J.-M., 2009. Mathematical modeling of the biofiltration of ethyl acetate and toluene and their mixture. Biochem. Eng. J. 43, 169–177. doi:10.1016/j.bej.2008.09.014

Álvarez-Hornos, F.J., Martínez-Soria, V., Marzal, P., Izquierdo, M., Gabaldón, C., 2017. Performance and feasibility of biotrickling filtration in the control of styrene

industrial air emissions. Int. Biodeterior. Biodegradation 119, 329–335. doi:10.1016/j.ibiod.2016.10.016

Arellano-García, L., Dorado, A.D., Morales-Guadarrama, A., Sacristan, E., Gamisans, X., Revah, S., 2015. Modeling the effects of biomass accumulation on the performance of a biotrickling filter packed with PUF support for the alkaline biotreatment of dimethyl disulfide vapors in air. Appl. Microbiol. Biotechnol. 99, 97–107. doi:10.1007/s00253-014-5929-7

Baltzis, B.C., Mpanias, C.J., Bhattacharya, S., 2001. Modeling the removal of VOC mixtures in biotrickling filters. Biotechnol. Bioeng. 72, 389–401. doi:10.1002/1097-0290(20000220)72:4<389::AID-BIT1001>3.0.CO;2-#

Baquerizo, G., Maestre, J.P., Sakuma, T., Deshusses, M.A., Gamisans, X., Gabriel, D., Lafuente, J., 2005. A detailed-model of a biofilter for ammonia removal: Model parameters analysis and model validation. Chem. Eng. J. 113, 205–214. doi:10.1016/j.cej.2005.03.003

Das, C., Chowdhury, R., Bhattacharya, P., 2011. Experiments and three phase modelling of a biofilter for the removal of toluene and trichloroethylene. Bioprocess Biosyst. Eng. 34, 447–458. doi:10.1007/s00449-010-0487-6

Derwent, R.G., Jenkin, M.E., Saunders, S.M., Pilling, M.J., 1998. Photochemical ozone creation potentials for organic compounds in northwest Europe calculated with a master chemical mechanism. Atmos. Environ. 32, 2429–2441. doi:10.1016/S1352-2310(98)00053-3

Deshusses, M.A., Webster, T.S., 2000. Construction and Economics of a Pilot/Full-Scale Biological Trickling Filter Reactor for the Removal of Volatile Organic Compounds from Polluted Air. J. Air Waste Manage. Assoc. 50, 1947–1956. doi:10.1080/10473289.2000.10464220

Devinny, J.S., Ramesh, J., 2005. A phenomenological review of biofilter models. Chem. Eng. J. 113, 187–196. doi:10.1016/j.cej.2005.03.005

Dorado, A.D., Baquerizo, G., Maestre, J.P., Gamisans, X., Gabriel, D., Lafuente, J., 2008. Modeling of a bacterial and fungal biofilter applied to toluene abatement: Kinetic parameters estimation and model validation. Chem. Eng. J. 140, 52–61. doi:10.1016/j.cej.2007.09.004

Dorado, A.D., Lafuente, J., Gabriel, D., Gamisans, X., 2012. Biomass accumulation in a biofilter treating toluene at high loads - Part 2: Model development, calibration and validation. Chem. Eng. J. 209, 670–676. doi:10.1016/j.cej.2012.08.019

European Union, 2010. Directive 2010/75/EU of the European Parliament and of the council of 24 November 2010 on industrial emissions (integrated pollution prevention and control) (Recast), Official Journal of the European Union.

Fan, L.-S., Leyva-Ramos, R., Wisecarver, K.D., Zehner, B.J., 1990. Diffusion of phenol through a biofilm grown on activated carbon particles in a draft-tube three-phase fluidized-bed bioreactor. Biotechnol. Bioeng. 35, 279–286. doi:10.1002/bit.260350309

Jorio, H., Brzezinski, R., Heitz, M., 2005. A novel procedure for the measurement of the kinetics of styrene biodegradation in a biofilter. J. Chem. Technol. Biotechnol. 80, 796–804. doi:10.1002/jctb.1245

Jorio, H., Payre, G., Heitz, M., 2003. Mathematical modeling of gas-phase biofilter performance. J. Chem. Technol. Biotechnol. 78, 834–846. doi:10.1002/jctb.835

Jung, I.G., Park, C.H., 2005. Characteristics of styrene degradation by Rhodococcus pyridinovorans isolated from a biofilter. Chemosphere 61, 451–456. doi:10.1016/j.chemosphere.2005.03.007

Kim, S., Deshusses, M.A., 2003. Development and experimental validation of a

490 conceptual model for biotrickling filtration of H2S. Environ. Prog. 22, 119–128.
491 doi:10.1002/ep.670220214
492 Lafita, C., Penya-Roja, J.-M., Gabaldón, C., Martínez-Soria, V., 2012. Full-scale
493 biotrickling filtration of volatile organic compounds from air emission in wood-
494 coating activities. J. Chem. Technol. Biotechnol. 87, 732–738.
495 doi:10.1002/jctb.3716
496 Lagarias, J.C., Reeds, J.A., Wright, M.H., Wright, P.E., 1998. Convergence Properties
497 of the Nelder-Mead Simplex Method in Low Dimensions. SIAM J. Optim. 9, 112–
498 147.
499 Liao, Q., Tian, X., Chen, R., Zhu, X., 2008. Mathematical model for gas-liquid two-
500 phase flow and biodegradation of a low concentration volatile organic compound
501 (VOC) in a trickling biofilter. Int. J. Heat Mass Transf. 51, 1780–1792.
502 doi:10.1016/j.ijheatmasstransfer.2007.07.007
503 Lim, J.S., Hwang, J.W., Choi, C.Y., Kim, B.H., Park, S., 2005. A pilot-scale rotating
504 drum biotrickling filter for removing gaseous styrene. Key Eng. Mater. 277–279,
505 517–522. doi:10.4028/www.scientific.net/KEM.277-279.517
506 Lu, C., 2001. Removal of styrene vapor from waste gases by a trickle-bed air biofilter.
507 J. Hazard. Mater. 82, 233–245. doi:10.1016/S0304-3894(00)00347-2
508 Mpanias, C.J., Baltzis, B.C., 1998. An experimental and modeling study on the removal
509 of mono-chlorobenzene vapor in biotrickling filters. Biotechnol. Bioeng. 59, 328–
510 43. doi:10.1002/(SICI)1097-0290(19980805)59:3<328::AID-BIT9>3.0.CO;2-D
511 National Toxicology Program (NTP), 2016. Report on Carcinogens, Fourteenth Edition.
512 Okkerse, W.J.H., Ottengraf, S.P.P., Osinga-Kuipers, B., Okkerse, M., 1999. Biomass
513 accumulation and clogging in biotrickling filters for waste gas treatment.
514 Evaluation of a dynamic model using dichloromethane as a model pollutant.

515 Biotechnol. Bioeng. 63, 418–430. doi:10.1002/(SICI)1097-
516 0290(19990520)63:4<418::AID-BIT5>3.0.CO;2-0
517 Parnian, P., Zamir, S.M., Shojaosadati, S.A., 2016. Effect of operating temperature on
518 styrene mass transfer characteristics in a biotrickling filter. Environ. Technol. 284,
519 926–933. doi:10.1080/09593330.2016.1226960
520 Pérez, M.C., Álvarez-Hornos, F.J., Portune, K., Gabaldón, C., 2015. Abatement of
521 styrene waste gas emission by biofilter and biotrickling filter: comparison of
522 packing materials and inoculation procedures. Appl. Microbiol. Biotechnol. 99,
523 19–32. doi:10.1007/s00253-014-5773-9
524 Reid, R.C., Prausnitz, J.M., Poling, B.E., 1987. The properties of gases and liquids.
525 McGraw-Hill Book Company, New York, EEUU.
526 San-Valero, P., Alcántara, S., Penya-Roja, J.M., Álvarez-Hornos, F.J., Gabaldón, C.,
527 2016. A Tool for Predicting the Dynamic Response of Biotrickling Filters for VOC
528 Removal. Chem. Eng. Commun. 203, 476–487.
529 doi:10.1080/00986445.2015.1025954
530 San-Valero, P., Gabaldón, C., Penya-roja, J.M., Quijano, G., 2017. Enhanced styrene
531 removal in a two-phase partitioning bioreactor operated as a biotrickling filter:
532 Towards full-scale applications. Chem. Eng. J. 309, 588–595.
533 doi:10.1016/j.cej.2016.10.054
534 San-Valero, P., Penya-Roja, J.M., Álvarez-Hornos, F.J., Gabaldón, C., 2014. Modelling
535 mass transfer properties in a biotrickling filter for the removal of isopropanol.
536 Chem. Eng. Sci. 108, 47–56. doi:10.1016/j.ces.2013.12.033
537 San-Valero, P., Penya-Roja, J.M., Álvarez-Hornos, F.J., Marzal, P., Gabaldón, C., 2015.
538 Dynamic mathematical modelling of the removal of hydrophilic VOCs by
539 biotrickling filters. Int. J. Environ. Res. Public Health 12, 746–766.

doi:10.3390/ijerph120100746

San-Valero, P., Penya-Roja, J.M., Sempere, F., Gabaldon, C., 2013. Biotrickling filtration of isopropanol under intermittent loading conditions. Bioprocess Biosyst. Eng. 36, 975–984. doi:10.1007/s00449-012-0833-y

Sander, R., 2005. Henry's law constants in NIST chemistry WebBook, NIST standard referencedatabase number 69, in: Linstrom, P.J., Mallard, W.G. (Eds.), National Institute of Standards and Technology. Gaithersburg MD 208999, USA.

Sempere, F., Gabaldón, C., Martínez-Soria, V., Marzal, P., Penya-roja, J.M., Alvarez-Hornos, F.J., 2008. Performance evaluation of a biotrickling filter treating a mixture of oxygenated VOCs during intermittent loading. Chemosphere 73, 1533–1539. doi:10.1016/j.chemosphere.2008.08.037

Sempere, F., Martínez-Soria, V., Palau, J., Penya-Roja, J.-M., San-Valero, P., Gabaldón, C., 2011. Effects of nitrogen source and empty bed residence time on the removal of styrene gaseous emissions by biotrickling filtration. Bioprocess Biosyst. Eng. 34, 859–67. doi:10.1007/s00449-011-0536-9

Shareefdeen, Z., Baltzis, B.C., Oh, Y.-S., Bartha, R., 1993. Biofiltration of methanol vapor. Biotechnol. Bioeng. 41, 512–524. doi:10.1002/bit.260410503

Webster, T.S., Cox, H.H.J., Deshusses, M.A., 1999. Resolving operational and performance problems encountered in the use of a pilot/full-scale biotrickling filter reactor. Environ. Prog. 18, 162–172. doi:10.1002/ep.670180312

Zarook, S.M., Shaikh, A.A., Ansar, Z., Baltzis, B.C., 1997. Biofiltration of volatile organic compound (VOC) mixtures under transient conditions. Chem. Eng. Sci. 52, 4135–4142. doi:10.1016/S0009-2509(97)00256-X

565 **Nomenclature**

a	Specific surface area of the packing material
C	Concentration
D	Diffusion coefficient
f(X_v)	Correction factor of diffusivity in the biofilm according to Fan's equation
H	Henry's law constant
K	Half saturation rate constant of the substrate
K_La	Overall mass transfer coefficient of the substrate
Q	Flow rate
p	Parameter
S	Concentration in the biofilm
t	Time
v	Superficial velocity
V	Volume
x	Coordinate for the depth in the biofilm
X_v	Biomass concentration in the biofilm
Y	Yield coefficient
z	Axial coordinate in the reactor from inlet to outlet
Greek letters	
β	Thickness of the liquid film
δ	Thickness of the biofilm
θ_B	Volume fraction occupied by the biofilm
θ_G	Porosity of the bioreactor
θ_L	Volume fraction occupied by the liquid film
θ_P	Void space of the packing material
μ_{max}	Maximum specific growth rate of the substrate
Subscripts	
i	Substance (styrene and oxygen)
d	Default
G	Gas
L	Liquid
B	Biofilm
Sty	Styrene
O	Oxygen
T	Tank
Z	Height of the reactor
Superscripts	
out	outlet

566

567